

---

# GRADIENT-BASED JOIN ORDERING

---

**Tim Schwabe**

Technical University of Munich

TUM School of Computation, Information and Technology

**Maribel Acosta**

Technical University of Munich

TUM School of Computation, Information and Technology

## ABSTRACT

Join ordering is the NP-hard problem of selecting the most efficient sequence in which to evaluate joins (conjunctive, binary operators) in a database query. As the performance of query execution critically depends on this choice, join ordering lies at the core of query optimization. Traditional approaches cast this problem as a discrete combinatorial search over binary trees guided by a cost model, but they often suffer from high computational complexity and limited scalability. We show that, when the cost model is differentiable, the query plans can be continuously relaxed into a soft adjacency matrix representing a superposition of plans. This continuous relaxation, together with a Gumbel-Softmax parameterization of the adjacency matrix and differentiable constraints enforcing plan validity, enables gradient-based search for plans within this relaxed space. Using a learned Graph Neural Network as the cost model, we demonstrate that this gradient-based approach can find comparable and even lower-cost plans compared to traditional discrete local search methods on two different graph datasets. Furthermore, we empirically show that the runtime of this approach scales linearly with query size, in contrast to quadratic or exponential runtimes of classical approaches. We believe this first step towards gradient-based join ordering can lead to more effective and efficient query optimizers in the future.

**Keywords** Join Ordering · Query Optimization · Graph Neural Networks · Knowledge Graphs

## 1 Introduction

Query optimization, particularly join ordering, is one of the most critical tasks in any database system. It involves determining the optimal evaluation sequence for the joins in a query, such that the resulting execution order has a low query runtime. Efficiently ordering join operations can significantly impact query execution time, often resulting in either instantaneous responses or impractically long delays.

At the core of join ordering is a *cost model*, which estimates the computational expense associated with executing a query or a part of it. Accurately estimating these costs is a challenging statistical estimation problem, primarily due to the complex data distributions and correlations within real-world databases. But, finding a good join ordering does not only involve estimating one query plan. It constitutes a discrete search problem over the space of plans, which are represented as binary trees, and which grows super-exponentially. Classical approaches to navigating this space typically rely on discrete methods like dynamic programming, which systematically evaluates possible plans at exponential cost, or greedy heuristics, which choose locally optimal steps fast but usually find suboptimal solutions.

Recently, learned cost models based on neural networks have been proposed, demonstrating significant superiority in cost estimation compared to classical statistical methods. However, these learned cost models are either still paired with traditional discrete search methods or completely rely on Reinforcement Learning, which is sample inefficient and has unstable convergence dynamics.

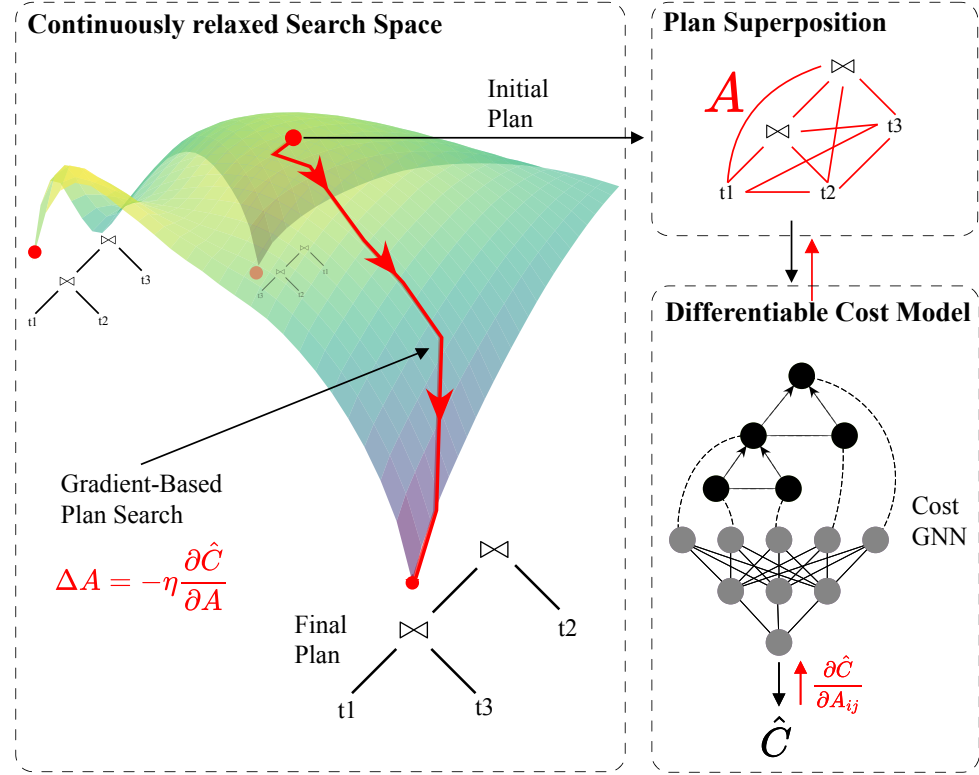


Figure 1: Join Ordering using a learned Cost Model. Continuously relaxing the discrete Search Space of Plans allows traversing it using Gradient Descent. The initial Plan is a superposition of all possible plans. The gradient search converges to a valid plan (the corners of the space) by minimizing the predicted cost.

In this work, we present a fundamentally different direction: we can exploit the differentiability of learned cost models and reformulate join ordering as a continuous optimization problem via relaxation of the discrete search space. As shown in Figure 1, we represent query plans as continuous adjacency matrices, enabling direct gradient-based search guided by a differentiable cost model. Therefore, the main contributions of this work are:

- We propose a novel gradient-based method for join ordering using learned cost models based on Graph Neural Networks, operating on a continuous relaxation of the discrete search space.
- We empirically show that this method generates solutions that approach and sometimes outperform ones found by discrete local search methods.
- We empirically show that the runtime of this approach is linear, as opposed to quadratic or exponential for discrete approaches.

## 2 Preliminaries

In this work, we assume a graph data model, where queries typically involve a large number of joins due to the fine-grained, triple-based representation of relationships. We assume basic familiarity with sets, graphs, and matrix notation.

### 2.1 Triple-Based Graph Queries

We assume a graph data model in which the data is stored as *triples*, i.e. labelled, directed edges

$$t = (s, p, o) \in \mathcal{E},$$

where each element belongs to a set  $s, p, o \in \mathcal{I}$ . A finite set of triples  $\mathcal{E}$  forms an edge-labelled directed graph.

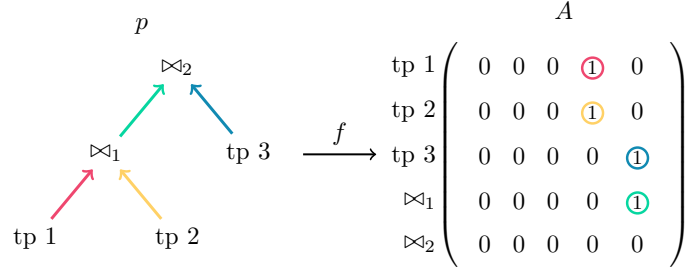


Figure 2: A join plan  $p$  is represented as a  $(2n - 1) \times (2n - 1)$  dimensional matrix  $f(p) = A$ . The first  $n$  rows denote the outgoing edges of triple patterns, while the last  $n - 1$  rows are outgoing edges of join nodes. The root node always corresponds to the last row.

**Triple patterns and conjunctive queries.** Such graphs are queried with *triple patterns*, i.e., triples in which any position may be a variable from an infinite set  $\mathcal{V}$  (s.t.  $\mathcal{V} \cap \mathcal{I} = \emptyset$ ) of *variables*:

$$tp = (s, p, o) \in (\mathcal{I} \cup \mathcal{V})^3.$$

A triple pattern is the most basic query. Its answer is the set of solution mappings

$$\Omega_{tp} = \{\mu : vars(tp) \rightarrow \mathcal{I} \mid \mu(tp) \in \mathcal{E}\},$$

where  $vars(tp)$  are the variables appearing in  $tp$ . The number of solution mappings is called the *cardinality*  $|\Omega_{tp}|$  of the triple pattern. More general *conjunctive queries* combine several triple patterns  $Q = \{tp_1, \dots, tp_n\} \subseteq (\mathcal{I} \cup \mathcal{V})^3$ .

**Join Operators.** The answer to a conjunctive query is obtained by iteratively *joining* the solution mappings. Let  $dom(\mu)$  denote the variables on which  $\mu$  is defined. Mappings  $\mu_1, \mu_2$  are *compatible*,  $\mu_1 \sim \mu_2$  if they assign the same value to every shared variable, i.e.  $\forall v \in dom(\mu_1) \cap dom(\mu_2) : \mu_1(v) = \mu_2(v)$ . Their union  $\mu_1 \cup \mu_2$  is the mapping with domain  $dom(\mu_1) \cup dom(\mu_2)$ . The join of two solution sets is then

$$\Omega_1 \bowtie \Omega_2 = \{\mu_1 \cup \mu_2 \mid \mu_1 \in \Omega_1, \mu_2 \in \Omega_2, \mu_1 \sim \mu_2\},$$

i.e., a set of solution mappings with cardinality  $|\Omega_1 \bowtie \Omega_2|$ .

## 2.2 Query Plans

The final set of solution mappings is invariant to the order in which the triple patterns are joined. However, since the number of intermediate results can differ vastly, the order still matters. A *query plan*  $p$  for  $Q$  defines the order in which these joins occur. Formally, it is a binary tree whose leaves correspond exactly to the triple patterns in  $Q$ , and internal nodes represent join operators combining intermediate results from their children.

- A plan is *bushy* if no structural restrictions exist. Joins may freely combine the results of arbitrary subplans.
- A plan is *left-linear* if each join operator has at most one non-leaf child. Such plans represent sequential join orders.

Since the space of bushy plans is vast ( $C_{n-1} n!$ , where  $C_{n-1}$  is the Catalan Number), commercial optimizers often restrict the search space to left-linear plans (with size  $n!$ ). While our proposed method is general and can search the space of bushy plans as fast as the space of left-linear plans, we focus on left-linear plans in this work. For a query with  $n$  triple patterns, we represent a plan  $p$  as an adjacency matrix  $A \in \{0, 1\}^{(2n-1) \times (2n-1)}$ , where  $A_{ij} = 1$  means node  $i$  is joined into node  $j$ . The first  $n$  indices in  $A$  correspond to triple patterns, and the last  $n - 1$  indices correspond to join nodes (see example in Figure 2).

## 2.3 Execution Cost and Cost Model

The goal of join ordering is to minimize the execution *cost* of a plan, which measures resources used, e.g., runtime, memory, disk access. Formally, the cost is defined as a function  $C : \mathcal{P} \rightarrow \mathbb{R}_{\geq 0}$ , mapping a plan  $p \in \mathcal{P}$  to its cost.

During optimization, a *cost model* is employed to approximate the true cost:

$$\hat{C}_\theta : \mathcal{P} \rightarrow \mathbb{R}_{\geq 0},$$

with parameters  $\theta$ . Simpler approaches rely on nonparametric statistical synopsises, while recent research often models  $\hat{C}_\theta$  using neural networks.

## 2.4 Cost Definition ( $C_{\text{out}}$ )

There are many options to define the cost of a query plan and its internal join operations. A popular definition of cost that is widely used and adopted in this paper is the so-called  $C_{\text{out}}$  cost function [1]. It recursively defines the cost of a join  $v$  as its output cardinality plus the costs of the left ( $l$ ) and right ( $r$ ) sides of the join:

$$C_{\text{out}}(v) = |\Omega(v)| + C_{\text{out}}(l) + C_{\text{out}}(r),$$

The cost of a leaf node (a triple pattern) is defined to be 0:

$$C_{\text{out}}(tp_i) = 0, \quad \text{for all leaves } tp_i.$$

## 2.5 Discrete Search Methods

In order to find a good join ordering, several search strategies are used. **Exhaustive Search (ES)** evaluates all possible plans and is guaranteed to find the optimum of the given cost model. However, its factorial complexity ( $\mathcal{O}(n!)$ ) for left-linear plans) makes it impractical beyond small queries.

**Dynamic Programming (DP)** reduces this to  $\mathcal{O}(3^n)$  by applying Bellman’s principle of optimality: the best plan for a set of joins can be built from optimal subplans [2]. However, this only works when the cost model satisfies this property and has no guarantees for arbitrary, non-monotonic cost models.

To circumvent the intractable time complexity for DP and ES, most optimizers make use of **Greedy Search**. At every iteration, the triple pattern (or intermediate sub-plan) whose addition locally yields the lowest estimated cost according to the cost model  $\hat{C}_\theta$  is appended to the join plan. Being a local search method, it can easily find suboptimal local optima. However, it only requires  $\mathcal{O}(n^2)$  evaluations of the cost model, making it computationally efficient.

## 3 Related Work

### Learned Cost Models

Traditional query optimizers rely on formula-based cost estimators that combine histograms, independence assumptions, and hand-crafted heuristics or sampling-based approaches, and are inaccurate for larger joins. Recent research, hence, turned to learned models to estimate the cardinality or cost of a query. These models try to map from a suitable representation of a query or plan to its cardinality or cost.

For relational data, *MSCN* [3] models tables, joins, and predicates with separate subnetworks that are aggregated to produce a cardinality estimate. To capture the inherent tree-based structure of query plans, several works use architectures such as Tree-LSTM [4], or Transformers [5] with tree-based attention.

For graph databases, several approaches have used GNNs [6, 7] or RNNs [8] and pretrained embeddings to accurately represent queries and estimate their cardinality. Similarly to approaches on relational databases, approaches for cost estimation explicitly represent the tree structure of the query plan [9, 10].

### Learned Query Optimization

The learned cardinality and cost estimators above can be used to search for optimal plans using greedy approaches or dynamic programming. To combine the time efficiency of greedy approaches with the ability to find more optimal plans of more exhaustive approaches, recent work has turned to reinforcement learning. The search for an optimal plan is cast as a Markov decision problem where the optimal next action is joining two subplans (where a subplan can be an unjoined table or triple pattern) such that the expected cost is minimized. Various approaches in relational and graph databases use common algorithms such as policy gradients [11] or Q-Learning [12, 13]. Similar to learned cost models, those approaches use Tree-based representations [13, 14] and Graph Neural Networks [12, 15] to represent the plans. Several surveys summarize the recent work in relational [16, 17] and graph databases [18].

Since RL approaches typically suffer from data-inefficient training, our approach focuses on cost models trained in a supervised way, offering dense feedback on costs and instead improving the search procedure to find better local minima than discrete search procedures.

### Gradient Based Optimization of Discrete Structures

Using Gradient Descent to optimize structures that are discrete in nature has been explored in various previous works and domains. *DARTS* [19] and *SNAS* [20] reformulate Neural Architecture Search to a smooth loss and use gradient descent to directly optimize the network architecture. The approach of *DART* is transferred to differentiable program synthesis by Cui et al. [21]. *NRI* [22] simultaneously learns the underlying discrete interaction graph and the dynamics

model of a dynamical system using GNNs inside an autoencoder. Structure learning, the task of finding the graph that best explains observed data, has also been approached using gradient-based optimisation [23, 24, 25]. In the space of control theory using learned world models, V et al. [26] perform gradient-based planning using a recurrent world model. In comparison to our work, they use gradient-based search to find a good order of actions to take, while we aim to find a good order of join operations.

*SNAS* and *NRI* both use the Gumbel-Softmax Trick [27], respectively Concrete Distribution [28] in order to obtain a differentiable approximation of sampling from a categorical distribution. In relation to this, Liu et al. [29] show how Gumbel-Softmax reparametrization can be used to solve combinatorial optimization problems on graphs using gradient descent.

Another line of work has applied continuous relaxation to the discrete process of sorting [30, 31, 32].

Despite these diverse approaches to gradient-based optimization in discrete search spaces, their application to query optimization remains unexplored, a gap that we aim to address in this work.

## 4 Gradient-Based Join Ordering

We now show how the search for an optimal plan can be reformulated using gradient descent. We first formalise the optimisation objective, then show how a continuous relaxation of the discrete plan space enables end-to-end gradient descent. Algorithm 1 shows the pseudocode of our approach.

### 4.1 Optimisation Objective

Given the set  $\mathcal{P}(Q)$  of possible plans for a query  $Q$ , i.e.  $\mathcal{P}(Q) \subseteq \mathcal{P}$ , and let  $f : \mathcal{P}(Q) \rightarrow \{0, 1\}^{N \times N}$  map a plan  $p$  to its binary adjacency matrix  $A_p = f(p)$ , where  $N = 2n - 1$  is the total number of plan nodes. Given a feature matrix  $X \in \mathbb{R}^{N \times F}$  with  $F$ -dimensional features for the nodes, and a differentiable cost model  $\hat{C}_\theta$ , join-ordering is the following discrete optimisation problem:

$$\min_{p \in \mathcal{P}(Q)} \hat{C}_\theta(X, f(p)). \quad (1)$$

### 4.2 Continuous Relaxation of Plans

To turn Equation (1) into a continuous problem, we relax the binary adjacency matrix  $A \in \{0, 1\}^{N \times N}$  by introducing a real-valued *logit matrix*  $L \in \mathbb{R}^{N \times N}$  and employing differentiable Gumbel-Softmax re-parameterisation [27]:

$$G_{ij} = -\ln(-\ln U_{ij}), \quad U_{ij} \sim \mathcal{U}(0, 1), \quad (2)$$

$$A^{\text{soft}} = \text{softmax}((L + G)/\tau), \quad (3)$$

where the softmax is applied row-wise.  $A^{\text{soft}}$  now represents a continuous superposition of discrete plans.

Since valid join plans are located at the binary vertices of the hypercube  $[0, 1]^{N \times N}$ , the optimisation must eventually drive each  $A_{ij}^{\text{soft}}$  towards either 0 or 1. This is achieved by annealing the temperature parameter  $\tau \in \mathbb{R}^+$  towards a minimum value  $\tau_{\min}$ . Specifically, the formulation using Gumbel-Softmax represents differentiable sampling from a Categorical Distribution over edges. As  $\tau \rightarrow 0$ , the entries of  $A_{ij}^{\text{soft}}$  approach binary values. To balance free exploration in early iterations with convergence towards discrete solutions in later stages, we linearly anneal the temperature over  $I$  optimization steps like  $\tau_t = \max(\tau_{\min}, \tau_0 - \frac{t}{I}(\tau_0 - \tau_{\min}))$ .

**Relaxed Optimisation Problem.** Relaxing the plan adjacency to continuous values now gives rise to a smooth objective

$$\min_{L \in \mathbb{R}^{N \times N}} \hat{C}_\theta(X, A^{\text{soft}}), \quad (4)$$

which can be approached using gradient-based methods.

### 4.3 Structural Constraints

Optimising Equation (4) alone empirically converges to degenerate minima, e.g., cyclic or disconnected graphs, that do not correspond to valid query plans. We therefore move to a constrained optimisation problem by adding differentiable penalties that quantify the invalidity of  $A^{\text{soft}}$  and vanish iff it is a valid, binary join tree.

**(i) Degree constraints.** We want to enforce that triple-pattern nodes have exactly one outgoing edge, while join nodes have exactly two incoming edges and one outgoing edge. Furthermore, the (single) root join node has no outgoing edges. Without loss of generality, let  $r = 2n - 1$  be the index of the root node. With in-degree  $d_v^{\text{in}} = \sum_i A_{iv}^{\text{soft}}$  and out-degree  $d_v^{\text{out}} = \sum_j A_{vj}^{\text{soft}}$ , we introduce quadratic penalties that are *zero iff* the degree conditions above are satisfied:

$$P_{\text{TO}} = \sum_{v \leq n} (d_v^{\text{out}} - 1)^2, \quad P_{\text{JI}} = \sum_{v > n} (d_v^{\text{in}} - 2)^2,$$

$$P_{\text{JO}} = (d_r^{\text{out}})^2 + \sum_{n < v < r} (d_v^{\text{out}} - 1)^2.$$

Note that we do not require a penalty for the in-degree of triple pattern nodes, as those can trivially be set to zero. While we penalize the out-degree of the root-node, we manually set it to 0 after optimization to override the softmax.

**(ii) Left-linearity.** The proposed method supports any bushy tree. However, it can be enforced to produce left-linear plans. For that, we require, without loss of generality (i) the first join node  $j_0$  (index  $n + 1$ ) to have two triple-pattern children and no join child, and (ii) every subsequent join node  $v \in J \setminus \{j_0\}$  to have exactly one triple-pattern child and one join child. With the sum of incoming connections from triple patterns  $c_v^{\text{tp}}$  and from join nodes  $c_v^{\text{in}}$  to  $v$  as

$$c_v^{\text{tp}} = \sum_{u \leq n} A_{uv}^{\text{soft}}, \quad c_v^{\text{in}} = \sum_{u > n} A_{uv}^{\text{soft}},$$

the left-linear penalty becomes

$$P_{\text{LL}} = (c_{j_0}^{\text{tp}} - 2)^2 + (c_{j_0}^{\text{in}})^2 + \sum_{v \in J \setminus \{j_0\}} [(c_v^{\text{tp}} - 1)^2 + (c_v^{\text{in}} - 1)^2].$$

Here  $J = \{n + 1, \dots, 2n - 1\}$  denotes the ordered set of join nodes. The penalty is zero iff the plan is left-linear.

**(iii) Acyclicity.** We discourage cycles via the matrix-exponential trace

$$P_{\text{ACYC}} = \text{tr}(e^{A^{\text{soft}}}) - N, \quad (5)$$

which is zero exactly for DAGs [23].

#### 4.4 Constrained Objective and Optimisation

Let  $P_{\text{STRUCT}} = \lambda_{\text{TO}} P_{\text{TO}} + \lambda_{\text{JI}} P_{\text{JI}} + \lambda_{\text{LL}} P_{\text{LL}} + \lambda_{\text{JO}} P_{\text{JO}} + \lambda_{\text{ACYC}} P_{\text{ACYC}}$  be the weighted sum of all structural penalties. The final time-dependent objective to be minimized is now given as

$$\mathcal{L}_t = \hat{C}_\theta(X, A^{\text{soft}}) + \lambda(t) P_{\text{STRUCT}}, \quad (6)$$

where  $\lambda(t) = \lambda_{\max}(t/I)^q$  nonlinearily increases the influence of the constraints over the  $I$  optimisation steps, up to a parameter  $\lambda_{\max}$ . Here, the exponent  $q$  is a hyperparameter. Similar to  $\tau$ , this allows for largely unconstrained exploration early on and forces valid plans at the end of optimization, and was empirically found to be critical for convergence.

The differentiability of both the cost model and the relaxed adjacency matrix makes  $\mathcal{L}_t$  amenable to standard gradient-descent updates:

$$L \leftarrow L - \alpha \nabla_L \mathcal{L}_t. \quad (7)$$

In practice, we use more efficient optimizers like AdamW. We dynamically retain the best plan encountered so far during optimization if  $P_{\text{STRUCT}} \leq \gamma$ , where  $\gamma$  is an empirically determined parameter.

**Projection to a Discrete Plan.** After the gradient-based search is completed, we convert the best found soft adjacency  $A^{\text{soft}}$  to a valid left-linear plan  $p^*$  by a simple best-first search: with  $T_{\text{free}} = \{1, \dots, n\}$ ,  $J_{\text{free}} = (n + 1, \dots, 2n - 1)$ , starting from the root join  $c = 2n - 1$  we iteratively select

$$(j^*, k^*) = \arg \max_{j \in T_{\text{free}}, k \in T_{\text{free}}} (A_{jc}^{\text{soft}} + A_{kc}^{\text{soft}}),$$

and attach the edges  $j^* \rightarrow c$  and  $k^* \rightarrow c$  to  $p^*$ , then set  $c \leftarrow j^*$  and  $T_{\text{free}} = T_{\text{free}} \setminus k^*$ ,  $J_{\text{free}} = J_{\text{free}} \setminus j^*$ ; the final join receives the two remaining triples. This projection is guaranteed to yield a valid plan. We choose it over a simple thresholding to 0 or 1, because in some rare cases the converged  $A^{\text{soft}}$  might not represent a valid plan. When it does, both thresholding and this projection result in the same plan.

**Algorithm 1** GRADIENT-BASED JOIN ORDERING

---

**Require:** node features  $X$ , trained cost model  $\hat{C}_\theta$ ,  
 iterations  $I$ , learning rate  $\alpha$ , exponent  $q$ , cap  $\gamma$ ,  
 temperatures  $(\tau_0, \tau_{\min})$ , penalty weights  $\{\lambda_k\}$

- 1: Initialise logits  $L_{ij} \sim \mathcal{U}[-0.05, 0.05]$ ,  
     set  $L_{ii} \leftarrow -\infty$
- 2:  $(L^*, C^*) \leftarrow (L, \infty)$
- 3: **for**  $t = 0$  **to**  $I - 1$  **do**
- 4:    $\tau \leftarrow \max(\tau_{\min}, \tau_0 - \frac{t}{I}(\tau_0 - \tau_{\min}))$
- 5:    $G_{ij} \leftarrow -\ln(-\ln U_{ij})$ ,  $U_{ij} \sim \mathcal{U}(0, 1)$
- 6:    $A^{\text{soft}} \leftarrow \text{softmax}((L + G)/\tau)$
- 7:    $\hat{c} \leftarrow \hat{C}_\theta(X, A^{\text{soft}})$
- 8:    $P_{\text{STRUCT}} \leftarrow \text{CALCPENALTY}(A^{\text{soft}}, \{\lambda_k\})$
- 9:    $\lambda(t) \leftarrow \lambda_{\max}(\frac{t}{I})^q$
- 10:    $\mathcal{L} \leftarrow \hat{c} + \lambda(t)P_{\text{STRUCT}}$
- 11:    $L \leftarrow \text{AdamW}(L, \nabla L \mathcal{L}, \alpha)$
- 12:   **if**  $\hat{c} < C^*$  **and**  $P_{\text{STRUCT}} < \gamma$  **then**
- 13:      $(L^*, C^*) \leftarrow (L, \hat{c})$
- 14: **return**  $p^* \leftarrow \text{PROJECTDISCRETE}(A^{\text{soft}})$

---

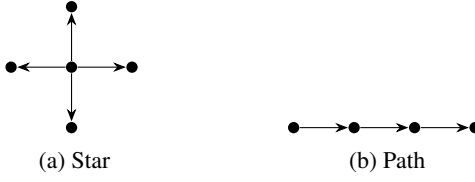


Figure 3: Examples of the used query shapes. Star queries have a single center node with multiple outgoing edges, while path queries form a single chain of connections.

## 5 Experimental Results

### 5.1 Datasets and Queries

We evaluate the proposed gradient-based optimization on two popular Knowledge Graphs: LUBM [33] and a subset of Wikidata (Wikidata 5M [34]). LUBM is a synthetic dataset used for Database Benchmarking, while Wikidata is one of the largest publicly available knowledge graphs. LUBM is a rather structured dataset, while Wikidata is complex and heterogeneous. Regarding queries, we use the star- and path-shaped queries provided by Schwabe et al. [6] and generate additional larger queries using their query generator. Star queries have a single central node that connects to various outer nodes, while a path query is a single chain of nodes (see Figure 3).

We selected these datasets and queries as they represent both smaller, simpler graphs as well as larger, more complex ones. The query shapes reflect those commonly studied in prior research and cover a wide range of cardinalities and costs, thus providing a representative range of typical query workloads. We use those queries to generate up to three random plans for each of them and then execute the queries against the database to obtain the  $C_{out}$  cost<sup>1</sup>.

To represent the feature matrix  $X$ , we yet again follow the same scheme as GNCE [6] and represent the subject, predicate, and object of a triple pattern using Knowledge Graph Embeddings. The full representation of a triple pattern is then the concatenation of the three embedding vectors (see the appendix for details).

### 5.2 Cost Model Training

Our approach is agnostic of model architecture and only expects the model to be compatible with a soft adjacency matrix. We choose a simple GNN with 3 message-passing layers and two fully connected layers, transforming the initial plan graph into a single cost estimate (details can be found in the appendix). As the message-passing function, we use *GIN Conv* [35] and extend it with edge weights in order to be able to represent the soft adjacencies. The GNN is trained on valid plans with hard adjacencies only to predict the  $C_{out}$  cost (details in the appendix).

<sup>1</sup>All used and generated datasets, as well as the code with instructions how to reproduce the results are available on GitHub: <https://github.com/TimEricSchwabe/GBJO>.

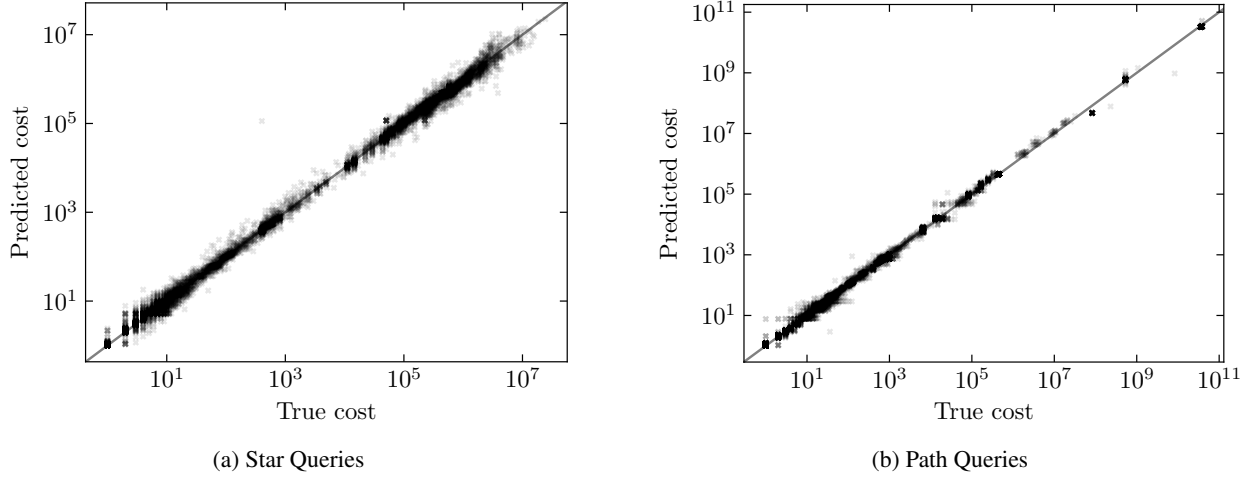


Figure 4: True vs. predicted costs for different query shapes (2–14 triple patterns) on the LUBM dataset.

For visualization, individual predictions for LUBM on the validation queries are shown in Figure 4. The number of plans used for training and validation along with the Q-error ( $\max(\frac{\hat{C}}{C}, \frac{C}{\hat{C}})$ ) between true ( $C$ ) and predicted ( $\hat{C}$ ) cost is shown in the table below.

	LUBM-Star	LUBM-Path	WD-Star	WD-Path
# Train	135699	41492	70743	9282
# Val	15078	4611	7861	1032
Q-error ↓	1.18	1.07	1.73	16.9

For both LUBM and Wikidata, and both query types, the models are reasonably estimating the cost. The performance on Wikidata path queries is worse since only 9k queries are used for training.

### 5.3 Join Order Optimization

We use the cost models trained in the previous step to compare the gradient-based search against the discrete greedy search. Both search methods, hence, use the exact same model. As explained, the Gradient-based Search is general and searches the space of bushy plans by default. We, however, decided to focus on left-linear plans only first. I.e., the left-linear penalty described above is used. Most of the hyperparameters, as shown in Algorithm 1, are rather robust to changes in their values (as determined using a Bayesian hyperparameter search). The most important hyperparameter was to gradually increase the penalties as opposed to them being applied completely from the beginning (Equation 6). The default values for the hyperparameters are  $I = 1000$ ,  $\alpha = 1.5$ ,  $\lambda_k = 2000$ ,  $\tau_0 = 5$ ,  $\tau_{\min} = 1$ ,  $\gamma = 5$ ,  $q = 7$ .<sup>2</sup> We further adopt the common assumption in join order optimization that the cost model is perfect and analyze the best found *predicted cost* of the optimization approaches. This isolates search quality from cost-estimation error.

#### 5.3.1 Visualizing the Cost Landscape

To verify that the learned cost model produces a well-behaved landscape outside the set of discrete plans on which it was trained, we visualise the predicted cost along one-dimensional trajectories that linearly interpolate between two randomly chosen valid plans  $P_1$  and  $P_2$ . Concretely, for a mixing coefficient  $\alpha \in [0, 1]$  we evaluate the model on the soft adjacency matrix  $A(\alpha) = (1 - \alpha)P_1 + \alpha P_2$  and plot both the predicted cost and structural penalty. Figure 5 shows these trajectories for star queries with 3, 8, and 14 triple patterns on the LUBM benchmark. Across all query sizes, the curves are smooth, without excessive nonlinearities, and, most importantly, the gradient at  $\alpha = 0.5$  consistently points towards the cheaper of the two endpoints.

This indicates that, even though the model has never been exposed to such invalid adjacency matrices during training, the relaxed landscape provides meaningful directional information for gradient-based optimisation. Lastly, the introductory Figure 1 shows a 3-D interpolation between all possible plans for a 3-tp query on LUBM, also confirming the smoothness and meaningfulness of the relaxed space.

<sup>2</sup>The Appendix provides the exact values and the tried ranges.

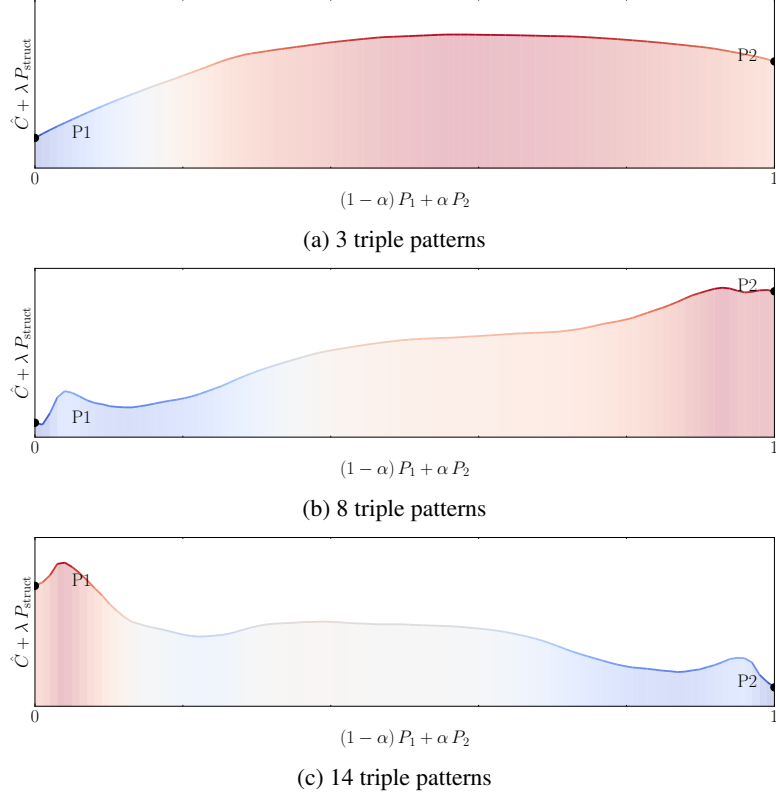


Figure 5: 1-D projections of the cost landscape between two random plans. Even though the space between plans does not represent valid plans, the local gradient still contains directional information towards the better plan.

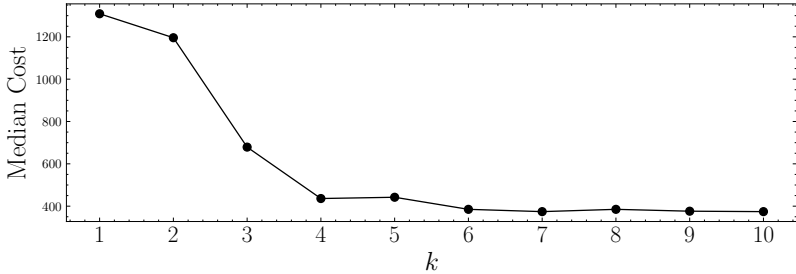


Figure 6: Increasing the number of gradient search fronts  $k$  quickly reduces the predicted cost of found plans.

### 5.3.2 Number of Search Fronts $k$

Performing a single gradient descent search quickly commits the optimizer to exploring one specific region of the search space, potentially limiting its ability to find better plans located elsewhere. To investigate whether introducing multiple parallel gradient descent search fronts improves the quality of the resulting plan, we executed  $k$  independent gradient searches simultaneously for path queries on the LUBM dataset. We then selected the best plan among them per query.

Figure 6 illustrates the median cost of the best-found plans as  $k$  varies. Increasing the number of parallel search fronts rapidly decreases the median cost by approximately two-thirds. However, this improvement quickly plateaus around  $k = 4$ , with diminishing returns for additional parallel searches beyond this point. Multiple runs can be efficiently parallelized into one batch on GPU, and hence improve the quality of found plans with minimal overhead.

### 5.3.3 Comparison to Discrete Local Search

Finally, we evaluate how the gradient-based search compares to the discrete greedy search. Building on the previous findings, we evaluate both a single search (i.e.,  $k = 1$ ) and a variant with  $k = 5$  independent search fronts. Figure 7

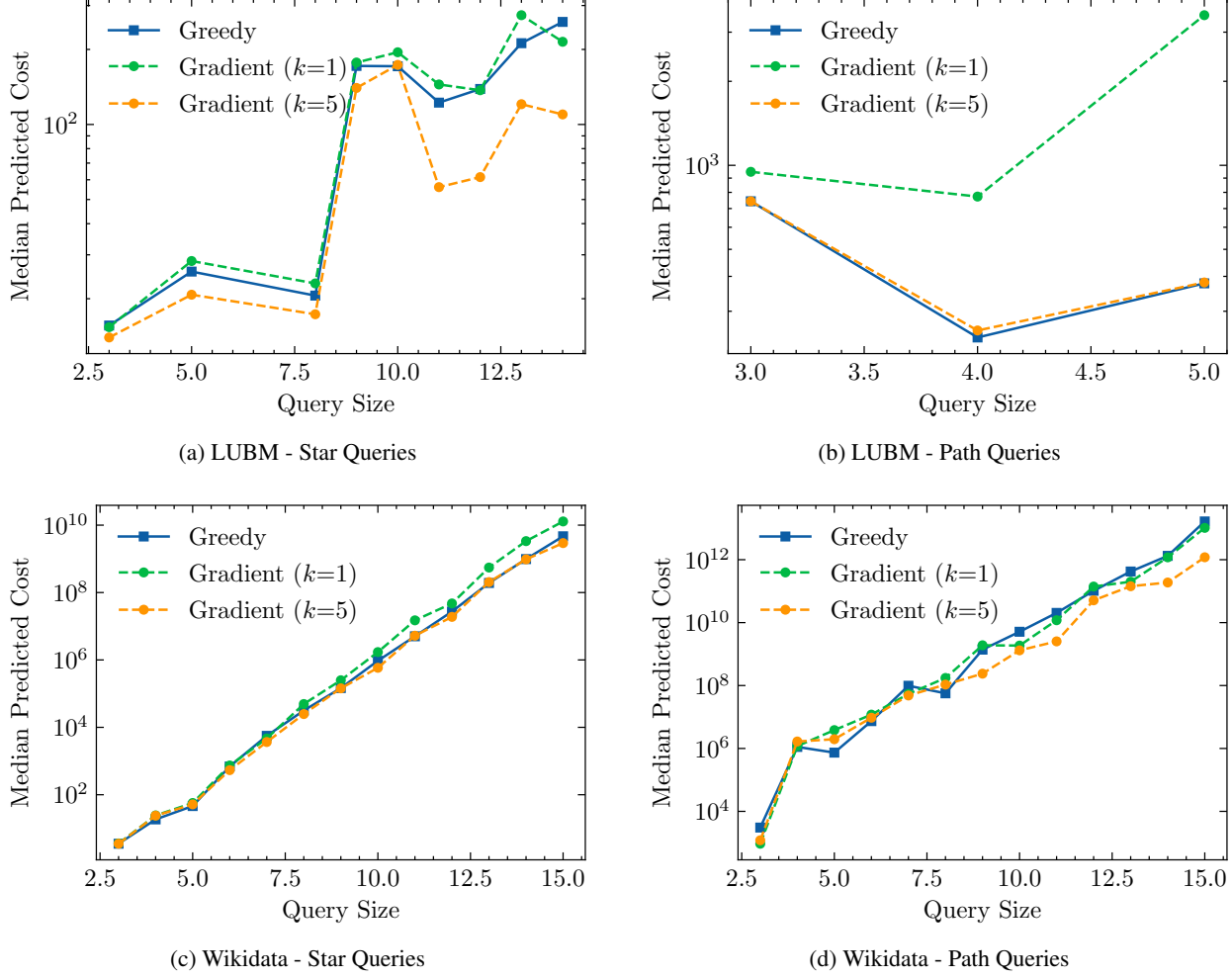


Figure 7: Predicted Costs of Plans found by Gradient- and Greedy-Search for LUBM and Wikidata.

compares the median predicted costs of plans produced by gradient searches with those obtained by discrete greedy search (GS) across increasing query sizes and for both star- and path-shaped queries on LUBM and Wikidata<sup>3</sup>.

With  $k = 1$ , the gradient search closely tracks the greedy baseline: for most query sizes, the costs of the two methods are comparable, showing that gradient-based search indeed converges to meaningful plans similar to discrete search. This behaviour is consistent across datasets and query shapes: neither the structural differences between star and path queries nor the heterogeneity of Wikidata versus the more regular LUBM schema materially affects the relative performance of gradient search, except for the LUBM path queries. Here, gradient search performs significantly worse. The reason for this might be that the search space is unfavorably shaped, and a single search might likely converge to a region of bad plans.

For  $k = 5$ , the gradient search improves over the discrete greedy search in most cases. For star queries on LUBM and path queries on Wikidata, the median predicted cost is significantly lower, especially for larger query sizes. For star queries on Wikidata, the predicted cost now matches or slightly improves over greedy search. For path queries on LUBM, the gradient search now coincides with greedy search.

Altogether, the results show that gradient-based join ordering can match and even improve its discrete counterpart. The gradient-based search can meaningfully traverse the continuous space of plan superpositions. This is intriguing since the cost model never saw plan superpositions during training, nor do they correspond to valid plans. As pointed out by Zhu et al. [36] for the task of continuous search in language modelling, this supports the idea that the gradient search

<sup>3</sup>We evaluated 20 queries per query size.

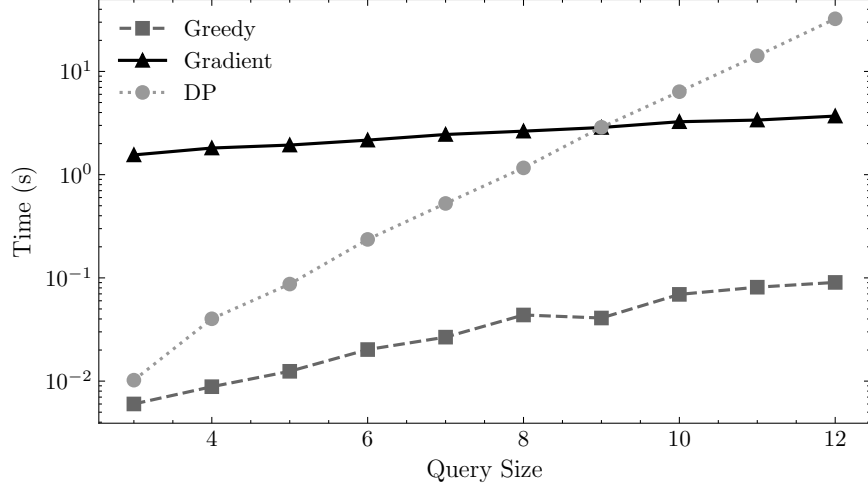


Figure 8: Search runtime. DP exhibits exponential and Greedy Search quadratic increase of runtime, while Gradient-Based Search scales linearly with query size.

implicitly explores multiple plans in parallel and can escape some of the local minima that the greedy search converges to.

#### 5.4 Runtime Performance

Figure 8 shows the wall-clock time w.r.t. query size for Dynamic Programming (DP), Greedy Search, and Gradient-Based Search (GBS) with  $I = 500$ , executed on CPU.

As initially stated, DP exhibits an exponential increase in runtime and GS a quadratic increase. In contrast, GBS shows a linear increase in runtime, which is a very favorable complexity behavior for a join order search method. The runtime is initially higher than DP and remains higher than GS, which is attributed to the fact that we perform a fixed number of forward and backward passes  $I$ . However, profiling shows that more than 80% of the runtime is attributed to the forward and backward passes. Hence, substantial improvements in absolute time are expected by compiling the forward and backward passes to static graphs and employing further runtime optimization techniques on GPU.

### 6 Limitations and Outlook

We demonstrated the feasibility of approaching join order optimization using gradient descent by continuously relaxing the discrete search over query plan trees. Our results indicate that gradient-based search can successfully find similar or better plans compared to discrete search methods.

Despite these promising results, several limitations remain. First, even though runtime scales linearly with query size, the proposed gradient-based method currently requires a relatively large number of forward and backward passes through the cost model, contributing significantly to the absolute runtime. This overhead could be reduced by employing optimized static computation graphs and more efficient GPU utilization techniques.

Second, the approach incorporates a significant number of hyperparameters. Converging to universal values for them across additional datasets and query shapes is important to enable easy application. Improving the algorithmic and architectural choices to require further gradient steps will also directly and significantly improve runtime.

Lastly, gradient descent is still inherently a local search and will find suboptimal plans. Combining gradient-based search with discrete approaches and Reinforcement Learning [26] is a promising direction to enhance the search quality.

### Acknowledgments

We thank Roman Mishchuk for valuable support in running experiments and for many helpful discussions about this work.

## References

- [1] Sophie Cluet and Guido Moerkotte. On the complexity of generating optimal left-deep processing trees with cross products. In Georg Gottlob and Moshe Y. Vardi, editors, *Database Theory - ICDT'95, 5th International Conference, Prague, Czech Republic, January 11-13, 1995, Proceedings*, volume 893 of *Lecture Notes in Computer Science*, pages 54–67. Springer, 1995.
- [2] Patricia G. Selinger, Morton M. Astrahan, Donald D. Chamberlin, Raymond A. Lorie, and Thomas G. Price. Access path selection in a relational database management system. In Philip A. Bernstein, editor, *Proceedings of the 1979 ACM SIGMOD International Conference on Management of Data, Boston, Massachusetts, USA, May 30 - June 1*, pages 23–34. ACM, 1979.
- [3] Andreas Kipf, Thomas Kipf, Bernhard Radke, Viktor Leis, Peter A. Boncz, and Alfons Kemper. Learned cardinalities: Estimating correlated joins with deep learning. In *9th Biennial Conference on Innovative Data Systems Research, CIDR 2019, Asilomar, CA, USA, January 13-16, 2019, Online Proceedings*. www.cidrdb.org, 2019.
- [4] Ji Sun and Guoliang Li. An end-to-end learning-based cost estimator. *Proc. VLDB Endow.*, 13(3):307–319, 2019.
- [5] Yue Zhao, Gao Cong, Jiachen Shi, and Chunyan Miao. Queryformer: A tree transformer model for query plan representation. *Proc. VLDB Endow.*, 15(8):1658–1670, 2022.
- [6] Tim Schwabe and Maribel Acosta. Cardinality estimation over knowledge graphs with embeddings and graph neural networks. *Proc. ACM Manag. Data*, 2(1):44:1–44:26, 2024.
- [7] Kangfei Zhao, Jeffrey Xu Yu, Hao Zhang, Qiyan Li, and Yu Rong. A learned sketch for subgraph counting. In Guoliang Li, Zhanhuai Li, Stratos Idreos, and Divesh Srivastava, editors, *SIGMOD '21: International Conference on Management of Data, Virtual Event, China, June 20-25, 2021*, pages 2142–2155. ACM, 2021.
- [8] Mehmet Aytürk, Theodoros Chondrogiannis, and Michael Grossniklaus. Space: Cardinality estimation for path queries using cardinality-aware sequence-based learning. *Proceedings of the ACM on Management of Data*, 3(3):1–26, 2025.
- [9] Daniel Casals, Carlos Buil-Aranda, and Carlos Valle. Sparql query execution time prediction using deep learning. 2023.
- [10] Abiram Mohanaraj, Matteo Lissandrini, Katja Hose, et al. Planrgcn: Predicting sparql query performance. *PROCEEDINGS OF THE VLDB ENDOWMENT*, 18(6):1621–1634, 2025.
- [11] Ryan Marcus and Olga Papaemmanouil. Deep reinforcement learning for join order enumeration. In Rajesh Bordawekar and Oded Shmueli, editors, *Proceedings of the First International Workshop on Exploiting Artificial Intelligence Techniques for Data Management, aiDM@SIGMOD 2018, Houston, TX, USA, June 10, 2018*, pages 3:1–3:4. ACM, 2018.
- [12] Jin Chen, Guanyu Ye, Yan Zhao, Shuncheng Liu, Liwei Deng, Xu Chen, Rui Zhou, and Kai Zheng. Efficient join order selection learning with graph-based representation. In Aidong Zhang and Huzefa Rangwala, editors, *KDD '22: The 28th ACM SIGKDD Conference on Knowledge Discovery and Data Mining, Washington, DC, USA, August 14 - 18, 2022*, pages 97–107. ACM, 2022.
- [13] Xiang Yu, Guoliang Li, Chengliang Chai, and Nan Tang. Reinforcement learning with tree-lstm for join order selection. In *36th IEEE International Conference on Data Engineering, ICDE 2020, Dallas, TX, USA, April 20-24, 2020*, pages 1297–1308. IEEE, 2020.
- [14] Ryan Marcus, Parimarjan Negi, Hongzi Mao, Chi Zhang, Mohammad Alizadeh, Tim Kraska, Olga Papaemmanouil, and Nesime Tatbul. Neo: A learned query optimizer. *Proc. VLDB Endow.*, 12(11):1705–1718, 2019.
- [15] Tianyi Chen, Jun Gao, Hedui Chen, and Yaofeng Tu. LOGER: A learned optimizer towards generating efficient and robust query execution plans. *Proc. VLDB Endow.*, 16(7):1777–1789, 2023.
- [16] Zhengtong Yan, Valter Uotila, and Jiaheng Lu. Join order selection with deep reinforcement learning: Fundamentals, techniques, and challenges. *Proc. VLDB Endow.*, 16(12):3882–3885, 2023.
- [17] Rong Zhu, Lianggui Weng, Bolin Ding, and Jingren Zhou. Learned query optimizer: What is new and what is next. In Pablo Barceló, Nayat Sánchez-Pi, Alexandra Meliou, and S. Sudarshan, editors, *Companion of the 2024 International Conference on Management of Data, SIGMOD/PODS 2024, Santiago, Chile, June 9-15, 2024*, pages 561–569. ACM, 2024.
- [18] Maribel Acosta, Chang Qin, and Tim Schwabe. *Neuro-Symbolic Query Optimization in Knowledge Graphs*. IOS Press, March 2025.

- [19] Hanxiao Liu, Karen Simonyan, and Yiming Yang. DARTS: differentiable architecture search. In *7th International Conference on Learning Representations, ICLR 2019, New Orleans, LA, USA, May 6-9, 2019*. OpenReview.net, 2019.
- [20] Sirui Xie, Hehui Zheng, Chunxiao Liu, and Liang Lin. SNAS: stochastic neural architecture search. In *7th International Conference on Learning Representations, ICLR 2019, New Orleans, LA, USA, May 6-9, 2019*. OpenReview.net, 2019.
- [21] Guofeng Cui and He Zhu. Differentiable synthesis of program architectures. In Marc'Aurelio Ranzato, Alina Beygelzimer, Yann N. Dauphin, Percy Liang, and Jennifer Wortman Vaughan, editors, *Advances in Neural Information Processing Systems 34: Annual Conference on Neural Information Processing Systems 2021, NeurIPS 2021, December 6-14, 2021, virtual*, pages 11123–11135, 2021.
- [22] Thomas N. Kipf, Ethan Fetaya, Kuan-Chieh Wang, Max Welling, and Richard S. Zemel. Neural relational inference for interacting systems. In Jennifer G. Dy and Andreas Krause, editors, *Proceedings of the 35th International Conference on Machine Learning, ICML 2018, Stockholmsmässan, Stockholm, Sweden, July 10-15, 2018*, volume 80 of *Proceedings of Machine Learning Research*, pages 2693–2702. PMLR, 2018.
- [23] Xun Zheng, Bryon Aragam, Pradeep Ravikumar, and Eric P. Xing. Dags with NO TEARS: continuous optimization for structure learning. In Samy Bengio, Hanna M. Wallach, Hugo Larochelle, Kristen Grauman, Nicolò Cesa-Bianchi, and Roman Garnett, editors, *Advances in Neural Information Processing Systems 31: Annual Conference on Neural Information Processing Systems 2018, NeurIPS 2018, December 3-8, 2018, Montréal, Canada*, pages 9492–9503, 2018.
- [24] Ignavier Ng, AmirEmad Ghassami, and Kun Zhang. On the role of sparsity and DAG constraints for learning linear dags. In Hugo Larochelle, Marc'Aurelio Ranzato, Raia Hadsell, Maria-Florina Balcan, and Hsuan-Tien Lin, editors, *Advances in Neural Information Processing Systems 33: Annual Conference on Neural Information Processing Systems 2020, NeurIPS 2020, December 6-12, 2020, virtual*, 2020.
- [25] Matthew J. Vowels, Necati Cihan Camgöz, and Richard Bowden. D'ya like dags? A survey on structure learning and causal discovery. *ACM Comput. Surv.*, 55(4):82:1–82:36, 2023.
- [26] Jyothir S. V. Siddhartha Jalagam, Yann LeCun, and Vlad Sobal. Gradient-based planning with world models. *CoRR*, abs/2312.17227, 2023.
- [27] Eric Jang, Shixiang Gu, and Ben Poole. Categorical reparameterization with gumbel-softmax. In *5th International Conference on Learning Representations, ICLR 2017, Toulon, France, April 24-26, 2017, Conference Track Proceedings*. OpenReview.net, 2017.
- [28] Chris J. Maddison, Andriy Mnih, and Yee Whye Teh. The concrete distribution: A continuous relaxation of discrete random variables. In *5th International Conference on Learning Representations, ICLR 2017, Toulon, France, April 24-26, 2017, Conference Track Proceedings*. OpenReview.net, 2017.
- [29] Jing Liu, Fei Gao, and Jiang Zhang. Gumbel-softmax optimization: A simple general framework for combinatorial optimization problems on graphs. In Hocine Cherifi, Sabrina Gaito, José Fernando Mendes, Esteban Moro, and Luis Mateus Rocha, editors, *Complex Networks and Their Applications VIII - Volume 1 Proceedings of the Eighth International Conference on Complex Networks and Their Applications COMPLEX NETWORKS 2019, Lisbon, Portugal, December 10-12, 2019*, volume 881 of *Studies in Computational Intelligence*, pages 879–890. Springer, 2019.
- [30] Aditya Grover, Eric Wang, Aaron Zweig, and Stefano Ermon. Stochastic optimization of sorting networks via continuous relaxations. In *7th International Conference on Learning Representations, ICLR 2019, New Orleans, LA, USA, May 6-9, 2019*. OpenReview.net, 2019.
- [31] Gwénolé Lecorvé, Morgan Veyret, Quentin Brabant, and Lina Maria Rojas-Barahona. Sparql-to-text question generation for knowledge-based conversational applications. In Yulan He, Heng Ji, Yang Liu, Sujian Li, Chia-Hui Chang, Soujanya Poria, Chenghua Lin, Wray L. Buntine, Maria Liakata, Hanqi Yan, Zonghan Yan, Sebastian Ruder, Xiaojun Wan, Miguel Arana-Catania, Zhongyu Wei, Hen-Hsen Huang, Jheng-Long Wu, Min-Yuh Day, Pengfei Liu, and Rui Feng Xu, editors, *Proceedings of the 2nd Conference of the Asia-Pacific Chapter of the Association for Computational Linguistics and the 12th International Joint Conference on Natural Language Processing, AACL/IJCNLP 2022 - Volume 1: Long Papers, Online Only, November 20-23, 2022*, pages 131–147. Association for Computational Linguistics, 2022.
- [32] Sebastian Prillo and Julian Martin Eisenschlos. Softsort: A continuous relaxation for the argsort operator. In *Proceedings of the 37th International Conference on Machine Learning, ICML 2020, 13-18 July 2020, Virtual Event*, volume 119 of *Proceedings of Machine Learning Research*, pages 7793–7802. PMLR, 2020.
- [33] Yuanbo Guo, Zhengxiang Pan, and Jeff Heflin. LUBM: A benchmark for OWL knowledge base systems. *J. Web Semant.*, 3(2-3):158–182, 2005.

- [34] Xiaozhi Wang, Tianyu Gao, Zhaocheng Zhu, Zhengyan Zhang, Zhiyuan Liu, Juanzi Li, and Jian Tang. KEPLER: A unified model for knowledge embedding and pre-trained language representation. *Trans. Assoc. Comput. Linguistics*, 9:176–194, 2021.
- [35] Keyulu Xu, Weihua Hu, Jure Leskovec, and Stefanie Jegelka. How powerful are graph neural networks? In *7th International Conference on Learning Representations, ICLR 2019, New Orleans, LA, USA, May 6-9, 2019*. OpenReview.net, 2019.
- [36] Hanlin Zhu, Shibo Hao, Zhiting Hu, Jiantao Jiao, Stuart Russell, and Yuandong Tian. Reasoning by superposition: A theoretical perspective on chain of continuous thought. *CorR*, abs/2505.12514, 2025.
- [37] Petar Ristoski and Heiko Paulheim. Rdf2vec: RDF graph embeddings for data mining. In Paul Groth, Elena Simperl, Alasdair J. G. Gray, Marta Sabou, Markus Krötzsch, Freddy Lécué, Fabian Flöck, and Yolanda Gil, editors, *The Semantic Web - ISWC 2016 - 15th International Semantic Web Conference, Kobe, Japan, October 17-21, 2016, Proceedings, Part I*, volume 9981 of *Lecture Notes in Computer Science*, pages 498–514, 2016.
- [38] Richard Liaw, Eric Liang, Robert Nishihara, Philipp Moritz, Joseph E Gonzalez, and Ion Stoica. Tune: A research platform for distributed model selection and training. *arXiv preprint arXiv:1807.05118*, 2018.
- [39] Takuya Akiba, Shotaro Sano, Toshihiko Yanase, Takeru Ohta, and Masanori Koyama. Optuna: A next-generation hyperparameter optimization framework. In *Proceedings of the 25th ACM SIGKDD International Conference on Knowledge Discovery and Data Mining*, 2019.

## A Cost Model Details

### A.1 Join and Triple Pattern Representation

We represent a triple pattern  $tp$  using an embedding vector  $e_{tp}$ . It consists of a concatenation of the embeddings of the subject, predicate, and object of the triple pattern and an indicator dimension that this is a triple pattern node ( $i = 0$ ):

$$e_{tp} = e_s \| e_p \| e_o \| i.$$

For the individual embeddings, we follow the approach proposed by GNCE [6] and use *rdf2vec* [37] embeddings. These work similarly to *word2vec* embeddings and provide a high-dimensional semantic representation of the entity, encoding its neighborhood and function within the graph. We also add the *count*  $c$  of the entity to the embedding. The count represents the number of times the entity ( $s$ ,  $p$ , or  $o$ ) appears in the graph. This serves as a simple yet meaningful prior quantity to estimate cost, as it can represent an upper limit. In case an entity is a variable, all dimensions of the RDF2Vec embedding are set to 1. Finally, we prepend an indicator dimension  $v$  to the full embedding to signal that the entity is constant ( $v = 0$ ) or a variable ( $v = 1$ ). Altogether, we represent an entity  $x$  like

$$e_x = v \| e_{\text{rdf2vec}}(x) \| c.$$

We choose 100-dimensional vectors for RDF2Vec, hence a complete embedding for an entity is 102-dimensional. A full embedding for a triple pattern is then 307-dimensional. As join nodes carry no inherent information, they are represented as 307-dimensional vectors where the first 306 dimensions are set to 0 and the indicator dimension is set to  $i = 1$ .

### A.2 GNN Architecture

The GNN  $\hat{C}(X, A^{\text{soft}})$  we use to transform a plan representation into a cost estimate consists of three message passing layers based on the GIN message passing function, which is extended by accepting edge weights to account for the soft adjacency matrix. The output  $z_i^{(l)}$  for a node indexed with  $i$  in layer  $l$  is given by

$$\text{GIN}(z_i^{(l-1)}) = \text{MLP}^{(l)} \left( (1 + \epsilon^{(l)}) h_i^{(l-1)} + \sum_{j \in \mathcal{N}(i)} a_{ji}^{\text{soft}} h_j^{(l-1)} \right)$$

Here  $\epsilon^{(l)}$  is a (learnable) scalar,  $\mathcal{N}(i)$  the set of neighbours of node  $i$ , and  $\text{MLP}^{(l)}$  is a two-layer perceptron. The message-passing layers are extended with skip connections, layer norm, and dropout. A sum aggregation combines the final node embeddings, and 2 fully connected layers transform the aggregation into a positive cost estimate:

$$\begin{aligned} x^{(0)} &= x \\ z^{(1)} &= \text{GIN}^{(1)}(x^{(0)}, A^{\text{soft}}) \\ x^{(1)} &= \text{Drop}(\text{ReLU}(\text{LN}(z^{(1)} + W_{\text{proj}} x^{(0)}))) \\ z^{(2)} &= \text{GIN}^{(2)}(x^{(1)}, A^{\text{soft}}) \\ x^{(2)} &= \text{Drop}(\text{ReLU}(\text{LN}(z^{(2)} + x^{(1)}))) \\ z^{(3)} &= \text{GIN}^{(3)}(x^{(2)}, A^{\text{soft}}) \\ x^{(3)} &= \text{ReLU}(\text{LN}(z^{(3)} + x^{(2)})) \\ h &= \sum_i x_i^{(3)} \\ g &= \text{Drop}(\text{ReLU}(W_1 h + b_1)) \\ \hat{C}(X, A^{\text{soft}}) &= |W_2 g + b_2| \end{aligned}$$

Here, LN denotes the layer norm, DROP the dropout,  $W_{\text{proj}}$ ,  $W_1$ ,  $W_2$  are linear matrices and  $b_1$  and  $b_2$  are bias vectors. For all tested models, we choose a hidden size  $x^{(i)}$  of 512.

### A.3 Training Procedure

The GNN is implemented using Pytorch Geometric. One model is trained per dataset and query shape with as many training plans as mentioned in the experimental section. All models are trained for 200 epochs using a batch size of 128 with the Adam optimizer using a learning rate of  $1e-4$ . As a loss function, the mean squared error between the predicted and true cost of a plan is used. The final model is chosen based on the lowest Q-Error on the validation plans.

Table 1: Final hyperparameters used for gradient-based join ordering, determined using Bayesian hyperparameter search.

	LUBM-Star	LUBM-Path	Wikidata-Star	Wikidata-Path
$I$	500	1000	1000	1000
$\alpha$	1.7	1.8	1	0.5
$\lambda_{ACYC}$	3081	4415	3391	467
$\lambda_{TO}$	135	790	2026	3661
$\lambda_{JI}$	1742	2197	2150	1919
$\lambda_{JO}$	1558	2204	1295	1900
$\lambda_{LL}$	2300	1910	2157	759
$q$	6.5	6.8	5.3	7
$\gamma$	5	8.6	3	0.5
$\tau_0$	4.5	3.7	15	5
$\lambda_{\max}$	2.6	4.2	0.7	1.8

## B Join Order Optimization - Hyperparameters

To choose the optimal hyperparameters of the gradient-based optimization, we performed a hyperparameter search per dataset and query type using the Ray Tune library [38] and the Optuna optimizer [39]. The results are shown in the parallel-coordinates plot in Figure 9. Per dataset, the hyperparameters are ordered with respect to their correlation with the mean predicted cost. While the relative importances differ between datasets, most variations of hyperparameters don't have a significant influence on the predicted cost, as indicated by the small correlation and the fact that good trials (color-coded in green) are distributed across the range of the parameter. However, for most datasets (except for Wikidata-Path), the usage of lambda ramping had the highest correlation, and almost all good trials use it. Other parameters that have a higher importance across datasets are  $\tau_0$  and  $p$ . While the hyperparameter search did not aid in finding a superior set of hyperparameters across datasets (or even individually within a dataset), the fact that for most parameters, good trials are scattered across the full range of the parameter demonstrates the robustness of the approach.

The final chosen hyperparameters are listed in Table 1. The ranges tried during hyperparameter search are specified in Table 2.

Table 2: Ranges of hyperparameters tried during hyperparameter optimization.

Parameter	Tried range / distribution
$I$	[100, 3000]
$\alpha$	[0.1, 100] — log-uniform
$\lambda_{ACYC}$	[ $10^2$ , $5 \times 10^3$ ] — uniform
$\lambda_{TO}$	[ $10^2$ , $5 \times 10^3$ ] — uniform
$\lambda_{JI}$	[ $10^2$ , $5 \times 10^3$ ] — uniform
$\lambda_{JO}$	[ $10^2$ , $5 \times 10^3$ ] — uniform
$\lambda_{LL}$	[ $10^2$ , $5 \times 10^3$ ] — uniform
<code>use_lambda_ramping</code>	{True, False} — categorical
$q$	[0.1, 10.0] — uniform
$\gamma$	[0.1, 10.0] — uniform
$\tau_0$	[1.0, 20.0] — uniform
$\lambda_{\max}$	[0.1, 5.0] — uniform

## C Hardware & Software

For the cost model training, we used a machine running Ubuntu with 16GB of RAM and an Nvidia T4 GPU. For the runtime and optimization experiments, a machine running Ubuntu with 16GB of RAM and Intel Core i7-1355U was used. The exact versions of the Python packages used are detailed in the requirements.txt of the code appendix.

This paper specifies the computing infrastructure used for running experiments (hardware and software), including GPU/CPU models; amount of memory; operating system; names and versions of relevant software libraries and frameworks.

## Gradient-Based Join Ordering

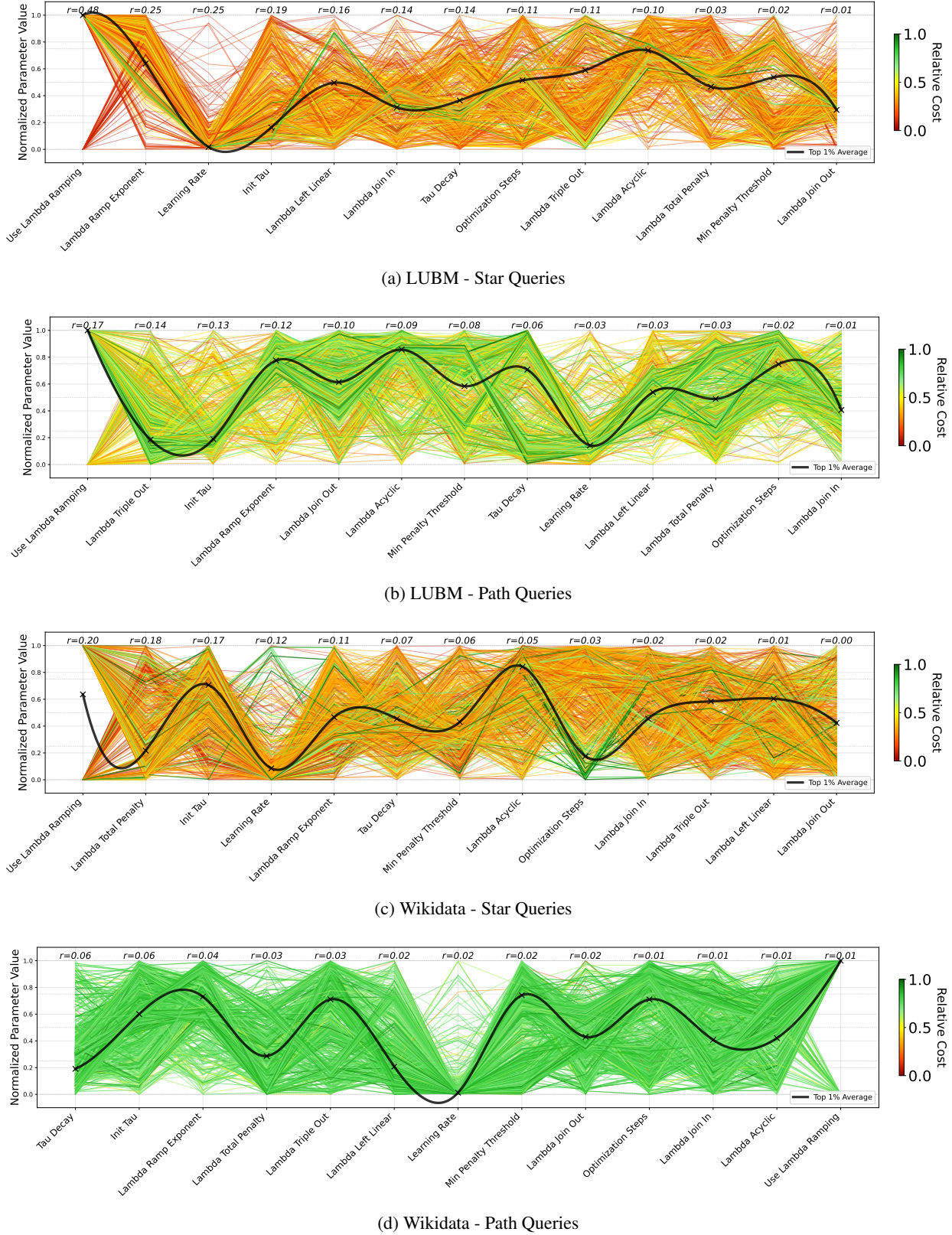


Figure 9: Results of the hyperparameter search for different datasets ordered with respect to their correlation with the mean predicted cost. Each line represents a single trial, color-coded by relative cost performance. The black line shows the average parameter values for the best 1% of trials.